Acta Cryst. (1995). D**51**, 711–717

Structure of the Azurin Mutant Nickel-Trp48Met from *Pseudomonas aeruginosa* at 2.2 Å Resolution

BY LI-CHU TSAI, LENNART SJÖLIN* AND VRATISLAV LANGER

Department of Inorganic Chemistry, Chalmers University of Technology and The University of Göteborg, S-412 96 Göteborg, Sweden

NICKLAS BONANDER, B. GÖRAN KARLSSON AND TORE VÄNNGÅRD

Department of Biochemistry and Biophysics, The University of Göteborg, S-412 90 Göteborg, Sweden

AND CHRISTIAN HAMMANN AND HERBERT NAR

Max Planck Institut für Biochemie, Abteilung fur Struktur Forschung, Martinsried bei München, Germany

(*Received* 18 *November* 1994; *accepted* 23 *January* 1995)

Abstract

The structure of the azurin mutant nickel-Trp48Met from *Pseudomonas aeruginosa* has been determined by difference Fourier synthesis using phases from the wild-type azurin model. The final crystallographic R value is 0.170 for 17 394 reflections to a resolution of 2.2 Å. The mutant crystallized in the orthorhombic space group $P2_12_12_1$, $a = 57.4$, $b = 80.4$, $c = 110.3$ Å. The four molecules in the asymmetric unit are packed as a dimer of dimers. The nickel metal site of this mutant structure is similar to the zinc metal site in the azurin Asp47 mutant. The site-specific mutation was performed at residue Trp48, which is located in the center of the protein in a highly hydrophobic environment, to investigate its suggested role in the long-range electron-transfer pathway between the disulfide bond on one side of the protein to the Cu centre. The structure around the mutation site Met48 showed no significant change compared with the wild-type structure.

Introduction

Azurin is a small cupredoxin ($M_r = 14\,000$) comprising a single polypeptide chain, which contains 128 amino-acid residues and one Cu atom. It is believed to accept an electron from cytochrome c_{551} (or from the bc_1 complex) and to deliver the electron to nitrite reductase. From a number of crystallographic studies of azurin (Adman, Stenkamp, Sieker & Jensen, 1978; Adman & Jensen, 1981; Baker, 1988; Nar, Messerschmidt, Huber, van de Kamp & Canters, 1991*a*; Tsai, Sjölin, Langer, Pacher & Nar, 1995) the copper site has been thoroughly determined. The Cu atom lies about 7 Å below the surface and is coordinated by five ligands, three equatorial ligands, His46, Cys112 and His117, and two weak ligands in axial positions, Gly45 and Met121. This geometry, the carbonyl O atom excepted, is conserved in all known structures of type I copper determined so far. The type I copper site found in azurin is spectroscopically characterized by an intense blue color and a narrow hyperfine coupling in the electron paramagnetic resonance (EPR) spectrum. In addition, it shows a high reduction potential compared to the aqueous Cu^{II}/Cu^{I} pair. The azurin molecule is built up by a short α-helix and eight β-strands. A general Greek-key motif is found in this protein, as well as in all other cupredoxins (Adman, 1991).

Electron transfer, in which azurin takes part, is one of the most important processes in living systems and occurs in many different reaction steps in respiration and photosynthesis and in other biochemical processes. It is commonly accepted that the physical mechanism for electron transfer in proteins is vibration-induced tunneling. Biological electron-transfer reactions then resemble inorganic redox reactions, and the relevant theory is mainly derived from the latter field (Marcus, 1957; Jortner, 1976; Marcus & Sutin, 1985). The structure-function relationships for electron transfer in blue-copper proteins have therefore attracted many investigators during recent years. Kinetic measurements, NMR studies, fluorescence anisotropy decays and crystallographic investigations have been used to explore the electron entrance site on the protein surface, as well as the electron exit site and plausible pathways (Lappin, Segal, Weatherburn & Sykes, 1979; Petrich, Longworth & Fleming, 1986; Tsai *et al.*, 1995). Electron-transfer theory for the long-range electron transfer in proteins involving electron tunneling through a polypeptide environment, has also been explored previously (Marcus & Sutin, 1985; Plato, Michel-Beyerle, Bixon & Jortner, 1989; Beratan, Betts & Onuchic, 1991; Farid, Moser & Dutton, 1993).

Recent biochemical and experimental investigations of the electron-transfer mechanism in azurin is in part

* Author for correspondence.

© 1995 International Union of Crystallography
Printed in Great Britain – all rights reserved

directed towards studies of intramolecular transfer rates in single-site mutated proteins. Azurin has only one tryptophan residue (Trp48), located in the center of the protein about 10 Å from the Cu atom, and, in addition, a single disulfide bridge (Cys3–Cys26) located at the end of strand 1 and strand 2, at a distance of 27 Å from the Cu atom (Nar, Messerschmidt, Huber, van de Kamp & Canters, 1991*b*). Azurin provides an excellent model system for studies of the intraprotein long-range electron transfer (LRET) from the disulfide to the Cu atom. Farver & Pecht (1989), using azurin as a model, proposed two pathways for the electron transfer from the disulfide bridge (Cys3–Cys26) to the copper ligands Cys112 and His46. In one of the electron-transfer pathways (from the disulfide to the Cys112 residue), the Trp48 side chain was assumed to be involved. In order to understand the role of this aromatic amino-acid residue, the single-site mutants Trp48Leu and Trp48Met, were also constructed and investigated (Farver *et al.*, 1993). This intramolecular electron-transfer reaction has, in addition, been examined with respect to the electronic coupling between the redox centers by calculating electronic factors using a tight-binding method for the two possible pathways (Broo & Larsson, 1991).

A crystal structure determination of the azurin mutant Trp48Met is, in this frame, a necessary complement to the interpretation of many aspects of the long-range electron-transfer pathway involving the Trp48 residue. This manuscript subsequently describes the crystallization, X-ray crystal analysis and refinement of the nickel-Trp48Met structure and in addition some of the biophysical properties of the *Pseudomonas aeruginosa* azurin mutant Trp48Met.

Materials and methods

Site-directed mutagenesis and preparation of P. aeruginosa azurins

The mutant was constructed with the use of the oligonucleotide-directed *in vitro* mutagenesis system. *Escherichia coli* K12 TG1 (Carter, 1986) was used for the DNA techniques. The plasmids pUC18/19 and M13mp18/19 were purchased from Boehringer-Mannheim. The plasmid pUG4 has been described by Karlsson, Pascher, Nordling, Arvidsson & Lundberg (1989). The azurin mutant was expressed in *E. coli* strain RV308 and fermented in 11 LB media, shake culture (16 h), and with ampicillin (100 $\mu g\, l^{-1}$) and isopropyl-β-D-thiogalactopyranoside (IPTG, 0.5 m*M*) added when the cultivation was started. The purification was carried out according to Karlsson *et al.* (1989) except that the sample was gel filtrated using a Sephadex S-100 gel in 100 m*M* phosphate pH 7.

Preparation of nickel-substituted azurin

The azurin mutant Trp48Met (~100 μM) was dialyzed against 0.1 *M* KCN in 20 m*M* Tris buffer pH 7.2 for 7 d. The sample was then transferred to 100 μM $NiCl_2$ in 20 m*M* Tris buffer at pH 7.2 and dialyzed against this solution for 7 d. The last step in the purification procedure of nickel-Trp48Met was anionic exchange chromatography on a Waters Q-8 HR column. Any remaining copper was then reduced with 100 m*M* ascorbic acid and the sample applied in 20 m*M* Tris–HCl buffer at pH 8.3, to which 100 μM $NiCl_2$ had been added, and eluted with a gradient of 0–80 mmol NaCl. These experiments were performed at room temperature. The fractions containing the nickel-Trp48Met were pooled and concentrated using an ultra-filtration unit and dialyzed against deionized water for 48 h at 277 K before the crystallization experiment.

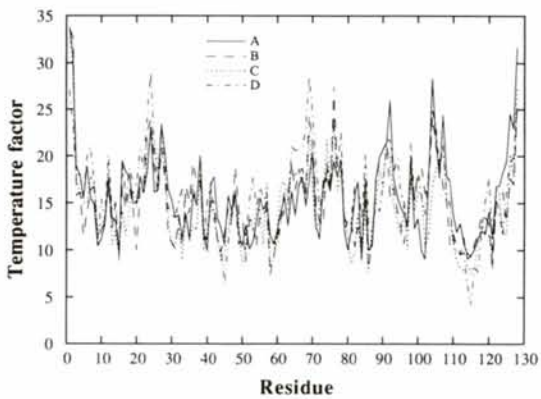

Fig. 1. Plot of temperature factors (Å^2) as a function of the amino-acid residue number for the four azurin mutant Trp48Met molecules in the asymmetric unit.

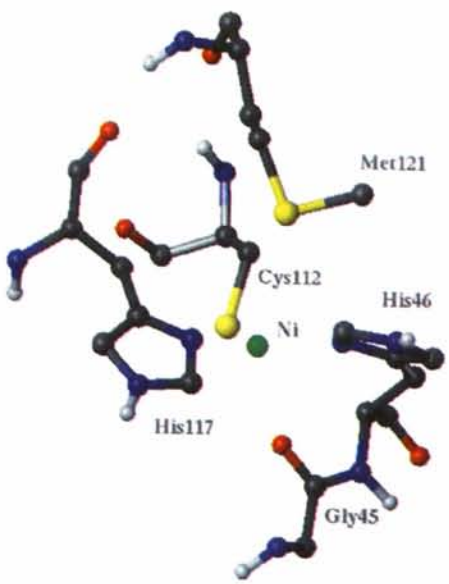

Fig. 2. The nickel site of the Ni-Trp48Met azurin with the planar and axial ligands shown.

Gel analysis

The sodium dodecyl sulfate polyacrylamide gel electrophoresis (SDS–PAGE) analysis was performed on a Pharmacia PhastSystem using Pharmacia SDS–PAGE gradient 8–25% gels. After the gel-filtration step the mutant appeared as a single band at 14 kDa on SDS–PAGE denaturing gel reduced with β-mercaptoethanol.

Optical and EPR spectra and reduction potentials

Optical spectra were recorded with a Shimadzu 3000 spectrophotometer. EPR spectra were obtained on a Bruker ER 20D-SRC spectrometer equipped with an Oxford Instrument using an EPR-9 helium cryostat. The optical spectra were recorded at a temperature of 293 K. Integrations were performed as described by Aasa & Vänngård (1975). All measurements were made in 100 m*M* KCl, 10 m*M* Hepes [4-(2-hydroxyethyl)-1-piperazineethanesulfonic acid], pH 7.0. The EPR parameters were taken from *S*-band spectra recorded at 77 K. The reduction potentials measured with the optically transparent thin-layer electrolysis technique were determined by Pascher, Karlsson, Nordling, Malmström & Vänngård (1993) at 298 K and using Tris(1,10-phenanthroline)cobalt(III) perchlorate as the redox mediator

Fig. 3. Stereoscopic view of the nickel metal site shown inside the electron density of the final $2F_o - F_c$ map which was contoured at 1σ level.

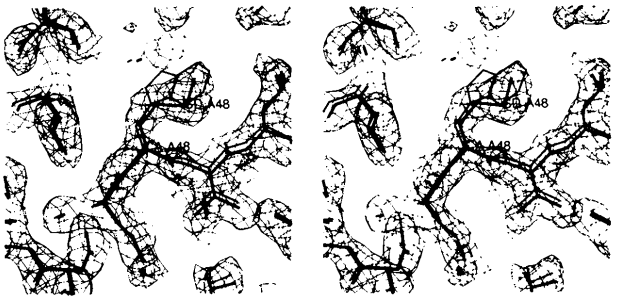

Fig. 4. Stereoscopic view of the mutation site Trp48Met with the wild-type coordinates superposed on the Ni-Trp48Met coordinates. The electron density from the final $2F_o - F_c$ map is also shown and contoured at 1σ level.

Table 1. *Data-collection parameters and statistics, the final model and refinement results for the nickel-Trp48Met mutant*

Unit-cell constants (Å)	*a*	57.4
	b	80.4
	c	110.3
Space group		$P2_12_12_1$
No. of molecules in the asymmetric unit		4
Crystal mosaicity (°)		0.19
Total No. of measurements		82349
Total No. of unique relfections		17974
Data completeness (%)		73
Reflection averaging (%) R_{merge}*		8.7
No. of atoms used in refinement		4210
Protein atoms		3872
Solvent		337
Nitrate ions		1
Resolution range used in the refinement (Å)		8.0–2.2
No. of reflections in the resolution range		17394
No. of parameters		16841
Root mean square deviations		
Bonds (Å)		0.015
Angles (°)		3.13
R value (%)†		17.0

* $R_{merge} = \sum\sum\langle I(H)\rangle - I(H)_i / \sum\sum I(H)_i$ where $I(H)_i$ is the *i*th intensity measurement of reflection *H*, $\langle I(H)\rangle$ is its mean value and the summation extends over all the reflections measured more than once in the set.

† $R = \sum |F_o - F_c| / \sum |F_o|$.

Crystallization and data collection

Prism-like yellowish nickel-Trp48Met crystals were formed from a solution containing 3.2 *M* ammonium sulfate, 1.0 *M* lithium nitrate and 0.2 *M* acetate buffer at pH 5.7 and at a temperature of 297–298 K in around 10 d. The largest crystal of this form was about 0.6 × 0.4 × 0.2 mm. This crystallization procedure is similar to the one used by Adman *et al.* (1978).

The diffraction data were collected from the largest crystal (0.6 × 0.4 × 0.2 mm) on a MicroVax III controlled FAST television area-detector diffractometer (Enraf–Nonius, Delft) in a thermostatically controlled room at 283 K. Cu $K\alpha$ radiation from a rotating-anode generator (Rigaku RU200, Japan) operating at 5.4 kW was used. From three frames of data collected as still photograms along the three reciprocal axes, the nickel-Trp48Met crystal was found to be isomorphous to the wild-type azurin protein with an orthorhombic space group $P2_12_12_1$. The cell constants were refined to be $a = 57.4$, $b = 80.4$, $c = 110.3$ Å, $V = 509\,000$ Å^3. A complete native data set was obtained by rotating the crystal 94° about the c^* axis. The rotation range was 0.1°. The reflection data (Table 1) were evaluated on-line using the program *MADNES* (Messerschmidt & Pflugrath, 1987). They were corrected for absorption effects using equivalent reflections to determine the absorption ellipsoid of the crystal by applying the program *ABSCOR* (Messerschmidt, Schneider & Huber, 1990) and merged and loaded using the program *PROTEIN* (Steigemann, 1974). The final data set after internal scaling consisted of 17 974 reflections and the completeness of the data

Table 2. *The completeness of the data (% observed) and the R_{merge} values (%) as a function of resolution* (Å)

Resolution (Å)	>4.31	3.42	2.99	2.71	2.52	2.37	2.25	2.15
Completeness	95.0	94.9	92.9	91.3	74.2	40.4	28.3	5.4
R_{merge} (%)	4.3	6.7	8.3	9.7	13.6	18.9	27.4	32.1

was 72.3%. The R_{merge} for individual measurements was 8.7% and R_{merge} as a function of resolution as well as the completeness of the data as a function of resolution are presented in Table 2. The overall B factor estimated from a Wilson plot (Wilson, 1949) was measured to be 18.3 Å^2. There are four molecules in the asymmetric unit and the calculated V_m value according to Matthews (1968) is 2.34 Å^3 Da^{-1}.

Structure solution and refinement

The structure of nickel-Trp48Met was determined by difference Fourier synthesis using phases from the wild-type azurin including water molecules and a nitrate molecule found in the wild-type structure but initially omitting atoms of residues 47–49. Crystallographic refinement was carried out with energy restraints using *X-PLOR* (Brünger, 1992). The nickel sites were refined without energy restraints. After a conjugate-gradient, energy-restrained positional refinement followed by a restrained B-factor refinement ($R = 22\%$), electron-density maps were calculated. The maps ($2F_o - F_c$ and $F_o - F_c$) were inspected and the coordinates were manually corrected on a graphics display (Evans & Sutherland) using the program *FRODO* (Jones, 1978). Particularly the coordinates from the water structure, initially adopted from the wild-type azurin structure, were inspected and waters were added or deleted according to indications in the Fourier map and, in addition, the formation of reasonable hydrogen bonds. The electron density at the mutation site showed a well defined position for the Met48 side chain. Trp48 was then exchanged for the methionine residue. During the subsequent conjugate-gradient, energy-restrained, positional and B-factor refinement the R value dropped to 17.0% using 17 394 reflections between 8.0 and 2.21 Å. In the final model the root-mean-square (r.m.s.) deviations from ideal geometry became 0.015 Å for bond lengths and 3.13° for bond angles. Non-crystallographic symmetry refinement was not utilized.

Results

The final model consists of 3872 atoms in four protein molecules, 337 water molecules and one nitrate ion. The final crystallographic R value is 17.0% for 17 394 reflections to 2.2 Å resolution. The average temperature factor for the protein atoms is 15.3 Å^2, the average temperature factor for the solvent atoms is 23.3 Å^2 and for all atoms the average temperature factor is 16.0 Å^2. This crystal form of the *P. aeruginosa* nickel-Trp48Met mutant contains 16 molecules in the unit cell. The four molecules in the asymmetric unit are packed as a dimer of dimers. The packing of the dimer in this mutant is almost identical to the dimer packing in the wild-type structure grown using the same precipitant and growth conditions.

A Ramachandran plot of the nickel-Trp48Met azurin mutant model was calculated and inspected and it was found to be nearly identical to Ramachandran plots calculated from the coordinates of the azurin mutants His35Leu and His35Gln and the coordinates from the zinc azurin mutant Asn47Asp (Nar *et al.*, 1991*a*; Sjölin *et al.*, 1993). A plot of the temperature factor (B) *versus* the residues was made to check for regions of high mobility as well as to indicate the quality of the structure after refinement (Fig. 1). A comparison of the

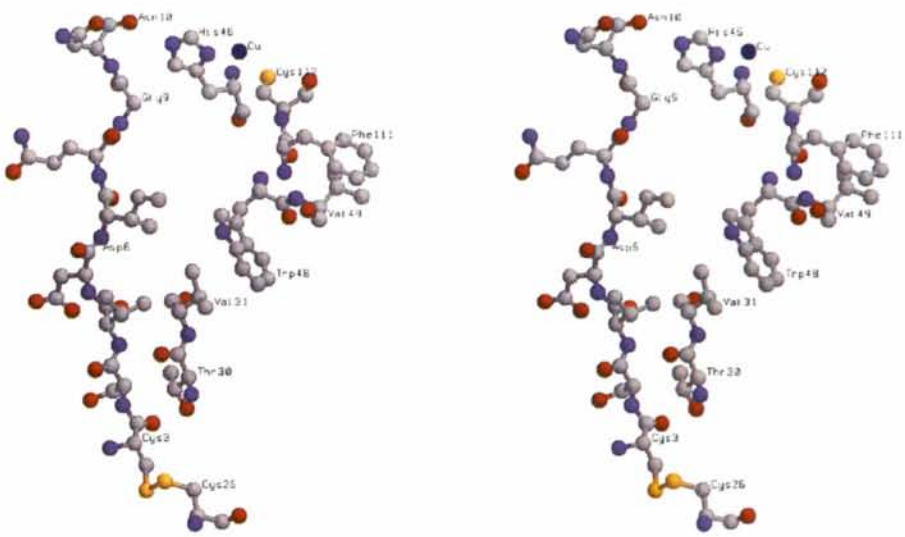

Fig. 5. A stereoscopic presentation of the backbone pathway, from Cys3 to His46 *via* Asn10, and the aromatic pathway from Cys3 to Cys112 through space jump Val31–Trp48, for long-range electron transfer in azurin.

Table 3. *The r.m.s. deviations calculated from a superposition of each of the four monomers A–D in the nickel-Trp48Met azurin mutant*

The four r.m.s. values per block (*A*) indicate values for C_α atoms, main-chain atoms, side-chain atoms and all atoms.

	A–B	*A–C*	*A–D*	*B–C*	*B–D*	*C–D*
C_α atoms	0.399	0.456	0.387	0.356	0.422	0.388
Main-chain atoms	0.448	0.506	0.407	0.354	0.480	0.381
Side-chain atoms	1.193	1.157	1.291	1.023	1.267	1.298
All atoms	0.881	0.814	0.934	0.747	0.937	0.957

Table 4. *The metal site geometry in the azurin mutant nickel-Trp48Met compared to wild-type azurin and zinc azurin*

Metal/ligand bond length (Å)	Ni-Trp48Met	Zn-Asn47Asp	Zn-azurin	wt-azurin
M—O(45)	2.35	2.36	2.32	2.97
M—N$^{\delta 1}$(46)	2.15	2.09	2.07	2.11
M—S$^{\gamma}$(112)	2.49	2.27	2.30	2.25
M—N$^{\delta 1}$(117)	2.07	2.04	2.01	2.03
M—S$^{\delta}$(121)	3.34	3.44	3.38	3.15
C$^{\alpha}$(45)—C$^{\alpha}$(121)	11.40	11.50	11.38	11.65
O(45)—C$^{\alpha}$(121)	9.09	9.19	9.09	9.42

four molecules in the asymmetric unit suggests that the deviation from the main-chain atom positions is small in the structure (Table 3).*

The metal coordination found in this mutant structure is similar to the metal coordination previously found in the Ni^{2+} wild-type azurin structure (Bonander *et al.*, 1995) and in the Zn^{2+} wild-type and Asn47Asp mutant structures (Nar *et al.*, 1992; Sjölin *et al.*, 1993). The nickel ion has a distorted tetrahedral coordination. Thus, it is coordinated by the four ligands, the atoms of O=C Gly45, Nδ His46, Sγ Cys112 and Nδ His117 (Table 4). The distance between the Ni atom and the Sδ Met121 is about 3.3 Å and must be regarded as a very weak bond (Fig. 2). An inspection of the $2F_o - F_c$ electron-density Fourier map at the nickel site reveals that the metal site and the ligands are very well defined (Fig. 3).

The site-specific mutation was introduced at Trp48 which is located in the center of the protein in a highly hydrophobic and rigid environment. The Trp48 residue is surrounded by the residues Ile7, Phe15, Ile20, Val31, Leu50, Phe97, Phe110 and Leu125. In the wild-type structure Val31 is very close to Trp48, with Cγ of Val31 at a distance of 3.93 Å from Cγ of Trp48. After the mutation Trp48Met, the Sδ of Met48 forms a weak hydrogen bond with NH of Val49 and with a distance of 3.4 Å. The distance between the Cγ of Val31 and the Cγ of Met48 in the mutant is 3.84 Å. The mutation Trp48Met resulted only in small differences between the mutant structure and the wild-type structure as can be found in Fig. 4. The Met48 amino-acid residue and its neighborhood are very well defined in the $2F_o - F_c$ Fourier map for the current structure.

Table 5. *Optical and EPR properties and reduction potentials of wild-type azurin, and mutants Trp48Leu and Trp48Met*

(*a*) Optical and EPR properties

$\mathbf{g}_\parallel$ and $\mathbf{g}_\perp$ are field vectors and $\mathbf{A}_\parallel$ is the hyperfine coupling in the parallel direction. ε is the optical absorption coefficient.

	EPR Parameters			λ_{max}	ε
Protein	$\mathbf{g}_\parallel$	$\mathbf{A}_\parallel$	$\mathbf{g}_\perp$	(nm)	(M^{-1} cm^{-1})
Wild type	2.259	50	2.059	627.0	5500
Trp48Leu	2.253	53	2.054	626.0	6800
Trp48Met	2.261	50	2.056	627.0	5400

(*b*) Reduction potentials

Protein	E° (mV) 0.2 *M* KCl, 10 m*M* Hepes* pH 7.0
Wild type	310
Trp48Leu	323
Trp48Met	312

* Hepes, 4-(2-hydroxyethyl)-1-piperazineethanesulfonic acid.

The spectroscopic characteristics of the copper-containing Met48 mutant indicated that the mutation in position 48 does not affect the copper site at all. Both the charge-transfer band and the EPR hyperfine splitting are almost identical to the wild-type protein. In addition, the reduction potential was measured to be 312 mV as compared to 310 mV in the wild-type protein. The spectroscopic and redox data are presented in more detail in Table 5.

Discussion

The copper-containing Met48 azurin mutant has also been crystallized from a solution containing PEG 4000 as a precipitant. X-ray diffraction data to 2.4 Å resolution have, in addition, been collected, but in spite of numerous attempts to solve the structure using rotation–translation function approaches we have not been able to find the solution. The reason for these difficulties was later determined to be crystal twinning. Since the Met48 azurin mutant did not crystallize in ammonium sulfate solution, we decided to exchange the Cu atom in the metal site for nickel since nickel-substituted azurin crystals were easily grown from an ammonium sulfate solution. We note that an exchange of copper for nickel did produce protein crystals of this mutant showing better quality and order. This approach is currently being introduced in the process of crystallizing plastocyanin from spinach, a protein and mutant system from which crystals have been notoriously difficult to obtain.

* Atomic coordinates and structure factors have been deposited with the Protein Data Bank, Brookhaven National Laboratory (Reference: 1NZR, R1NZRSF). Free copies may be obtained through The Managing Editor, International Union of Crystallography, 5 Abbey Square, Chester CH1 2HU, England (Reference: AB0335).

Another opportunity that emerges from the exchange of copper for nickel is the opportunity to verify the stability of the metal site since the stability is an essential prerequisite for the electron-transfer properties in small blue-copper proteins. According to the idea of the rack mechanism for proteins and enzymes (Lumry & Eyring, 1954) key functional groups can be held in distorted positions by the overall protein conformation, this in turn leading to anomalous properties. Experimental support for this concept has previously been obtained, particularly from investigations of metalloenzymes (Lindskog & Malmström, 1962). In all known structures of cupredoxins the Cu atom is bound at the same end of a β-barrel with one of its ligands, the histidine ring, exposed at the surface of the protein. A number of pathways for the electron to enter and to leave the copper have been suggested previously. These include, among others, a pathway through the so-called hydrophobic patch at the surface ligand His117 (Nar *et al.*, 1991*a*; Tsai *et al.*, 1995). In the metal site, the Ni atom has shifted slightly from the regular copper position to obtain a more pronounced tetrahedral coordination site. The Ni atom has, similar to the Zn and the Co atoms, moved towards the carbonyl O atom of Gly45 (Bonander *et al.*, 1995). The movement is accompanied by a small adjustment of the polypeptide chain in the neighborhood of Gly45. The other metal-liganding residues have maintained their normal positions, except Cys112 which has moved slightly. These features have also been found in the nickel-substituted azurin structure (Bonander *et al.*, 1995). Zinc binding to azurin also causes a structural adjustment of the polypeptide atoms in its immediate surroundings. Significant shifts were previously observed and reported for residues 44 and 45 (Nar *et al.*, 1992; Sjölin *et al.*, 1993). In particular, O45 moved about 0.3 Å towards the Zn atom making the metal cage compressed in the apical direction.

The main goal for the extensive research work on the electron-transfer problem in metalloproteins has been to explain the fast reaction between different proteins. One interesting question that can be raised is what evolution has done to make electron transfer possible and yet minimize the energy loss in the electron-transfer steps between different proteins in biological systems. Three important contributions are immediately recognized, the driving force of the reaction ($-\Delta G^\circ$), the reorganization energy λ and the electronic coupling, Δ. For a definition of the theoretical equation see, for instance, Larsson (1981).

The overall difference between the Ni-Trp48Met structure and the wild-type azurin structure is very small (Fig. 4). In the mutation site the methionine side chain is oriented in the direction of the Trp48 side chain in the wild-type structure. The structural differences in the neighborhood are also minute and within experimental error and we now assume, because of the lack of structural differences, that the reorganization energy has not changed since the Trp48Met mutant will probably behave like the wild-type azurin in terms of λ.

Farver & Pecht (1989) measured the electron transfer between the copper site in azurin and the sulfur bridge between Cys3 and Cys26. They suggested two possible pathways for the electron transfer, a 'backbone' way and an 'aromatic' way (Fig. 5). By using extended Hückel (EH) calculations Broo & Larsson (1991) initially found that the aromatic pathway gave a larger absolute Δ. However, calculations on several structures obtained from modeling of mutants did not give a clear picture of the role of the aromatic residues. The coupling decreased when the indole group of Trp48 was removed, but increased if, in addition, two other aromatic side chains Phe15 and Phe29 were also eliminated.

Farver *et al.* (1993) showed in a radiolysis experiment that when Trp48, situated midway between the donor and acceptor in the azurin system, was replaced by Leu or Met, only a small change in the rate of intramolecular electron transfer was observed, indicating in favor of the Broo & Larsson (1991) investigation that the aromatic residue in this position is only marginally involved in electron transfer in wild-type azurin. By using electron-pathway calculations according to Beratan, Betts & Onuchic (1992), Farver *et al.* (1993), in addition, showed that the longer through-backbone path is more efficient than the shorter one involving Trp48 (Fig. 5). The calculations by Farver *et al.* (1993) was based on coordinates modeled on the graphics display for the mutants Met48 and Leu48 since no X-ray structure data were available at that time. These coordinates were obtained by changing Trp48 for Met48 (or Leu48) and subsequently the new coordinate set was subjected to an energy minimization and molecular dynamics simulation using the programs *Discover* and *Insight* II (Biosym Technologies, San Diego, CA). When the resulting coordinates were compared to the coordinates from our X-ray structure by superposing one on top of the other we found that the r.m.s. difference for the main-chain atoms was 0.23 Å and the r.m.s. difference for the side-chain atoms was 0.42 Å. These differences are to be considered small. However, when inspecting the mutation site (Met48) one can find that the model coordinates follow closely the structure coordinates for the Cα, Cβ and the Cγ atoms but the Sδ sites differ by approximately 1.1 Å. The difference of 1.1 Å in the position of the Sδ atom is significant even though Cε differs only by 0.3 Å between the two models. Since this position is the crucial position for the Beratan calculations (determining the length of the through-space jump, Fig. 5) the small difference of about 0.3 Å would not have affected the results of the calculations significantly. This was confirmed in a supplementary Beratan calculation performed on the new coordinate set.

The various roles of the aromatic amino-acid residues tryptophan, phenylalanine and tyrosine for electron transfer in proteins in general is an important question

and evidently in some cases the aromatic amino acids may also serve as important functional components in the electron-transfer scheme (Plato *et al.*, 1989). In other cases as in azurin the Trp48 aromatic side chain seems to play a rather limited role for the intramolecular transfer rate. Farver *et al.* (1993) have suggested another mutant based on their results: Val31Trp in the proximity of Trp48 and in the electron-transfer path is thought to be very interesting since it is the through-space jump partner to Trp48 (Fig. 5). If this side chain is favourably packed it would create partial aromatic side-chain stacking in this region. Consequently an increase in the long-range electron-transfer rate should be found as a result of overlapping π-bonds. Preliminary results obtained from radiolysis experiment on this mutant by Farver, Israel, Vänngård, Young & Bonander (1995) have, in fact, indicated a tenfold increase in the electron-transfer rate. Mutations in the Trp48 site or its neighborhood will probably continue to be important to probe the characteristics of the electron transfer through bonds or through space jumps and subsequently probe their rate penalties. Crystallographic investigations will be continued in the study of the structural consequences of each mutation.

We would like to thank the Swedish Natural Science Research Council and the Bio-Väst Foundation for Biotechnology (Göteborg) for financial support of this project. Dr Bruno Källebring is acknowledged for the supplementary Beratan calculations.

References

AASA, R. & VÄNNGÅRD, T. (1975). *J. Magn. Res.* **19**, 308–315.

ADMAN, E. T. (1991). *Adv. Protein Chem.* **42**, 145–197.

ADMAN, E. T. & JENSEN, L. H. (1981). *Isr. J. Chem.* **21**, 8–12.

ADMAN, E. T., STENKAMP, R. E., SIEKER, L. C. & JENSEN, L. H. (1978). *J. Mol. Biol.* **123**, 35–45.

BAKER, E. N. (1988). *J. Mol. Biol.* **203**, 1071–1095.

BERATAN, D. N., BETTS, J. N. & ONUCHIC, J. N. (1991). *Science*, **252**, 1285–1288.

BERATAN, D. N., BETTS, J. N. & ONUCHIC, J. N. (1992). *J. Phys. Chem.* **96**, 2852–2855.

BONANDER, N., KARLSSON, B. G., VÄNNGÅRD, T., TSAI, L.-C., LANGER, V., SJÖLIN, L., HAMMANN, C. & NAR, H. (1995). In preparation.

BROO, A. & LARSSON, S. (1991). *J. Phys. Chem.* **95**, 4925–4928.

BRÜNGER, A. T. (1992). *X-PLOR, Version* 3.1. Yale Univ. Press, New Haven, CT, USA.

CARTER, P. (1986). *Biochem. J.* **237**, 1–7.

FARID, R. S., MOSER, C. C. & DUTTON, P. L. (1993). *Curr. Op. Struct. Biol.* **3**, 225–233.

FARVER, O., ISRAEL, S., VÄNNGÅRD, T., YOUNG, S. & BONANDER, N. (1995). In preparation.

FARVER, O. & PECHT, I. (1989). *Proc. Natl Acad. Sci. USA*, **86**, 6968–6975.

FARVER, O., SKOV, L. K., PASCHER, T., KARLSSON, B. G., NORDLING, M., LUNDBERG, L., VÄNNGÅRD, T. & PECHT, I. (1993). *Biochemistry*, **32**, 7317–7322.

JONES, T. A. (1978). *J. Appl. Cryst.* **11**, 268–272.

JORTNER, J. (1976). *J. Chem. Phys.* **64**, 4860–4867.

KARLSSON, B. G., PASCHER, T., NORDLING, M., ARVIDSSON, R. H. A. & LUNDBERG, L. G. (1989). *FEBS Lett.* **246**, 211–217.

LAPPIN, A. G., SEGAL, M. G., WEATHERBURN, D. C. & SYKES, A. G. (1979). *J. Am. Chem. Soc.* **101**, 2297–2301.

LARSSON, S. (1981). *J. Am. Chem. Soc.* **103**, 4034–4040.

LINDSKOG, S. & MALMSTRÖM, B. G. (1962). *J. Biol. Chem.* **237**, 1129–1137.

LUMRY, R. & EYRING, H. (1954). *J. Phys. Chem.* **58**, 110–120.

MARCUS, R. A. (1957). *J. Chem. Phys.* **26**, 867–872.

MARCUS, R. A. & SUTIN, N. (1985). *Biochim. Biophys. Acta*, **811**, 265–322.

MATTHEWS, B. W. (1968). *J. Mol. Biol.* **33**, 491–497.

MESSERSCHMIDT, A. & PFLUGRATH, J. W. (1987). *J. Appl. Cryst.* **20**, 306–315.

MESSERSCHMIDT, A., SCHNEIDER, M. & HUBER, R. (1990). *J. Appl. Cryst.* **23**, 436–439.

NAR, H., HUBER, R., MESSERSCHMIDT, A., FILIPPOU, A. C., BART, M., JAQUINOD, M., VAN DE KAMP, M. & CANTERS, G. W. (1992). *Eur. J. Biochem.* **205**, 1123–1129.

NAR, H., MESSERSCHMIDT, A., HUBER, R., VAN DE KAMP, M. & CANTERS, G. W. (1991*a*). *J. Mol. Biol.* **221**, 427–447.

NAR, H., MESSERSCHMIDT, A., HUBER, R., VAN DE KAMP, M. & CANTERS, G. W. (1991*b*). *J. Mol. Biol.* **221**, 765–776.

PASCHER, T., KARLSSON, B. G., NORDLING, M., MALMSTRÖM, B.G. & VÄNNGÅRD, T. (1993). *Eur. J. Biochem.* **207**, 1026–1034.

PETRICH, J. W., LONGWORTH, J. W. & FLEMING, G. R. (1986). *Springer Ser. Chem Phys.* **46**, 413–415.

PLATO, M., MICHEL-BEYERLE, M. E., BIXON, M. & JORTNER, J. (1989). *FEBS Lett.* **249**, 70–74.

SJÖLIN, L., TSAI, L.-C., LANGER, V., PASCHER, T., KARLSSON, B. G., NORDLING, M. & NAR, H. (1993). *Acta Cryst.* D**49**, 449–457.

STEIGEMANN, W. (1974). PhD thesis, Technische Univ., München, Germany.

TSAI, L.-C., SJÖLIN, L., LANGER, V., PASCHER, T. & NAR, H. (1995). *Acta Cryst.* D**51**, 168–176.

WILSON, A. J. C. (1949). *Acta Cryst.* **2**, 318–321.